

Synthesis and structural details of perovskites within the series $\text{PrCo}_{1-x}\text{Cr}_x\text{O}_3$ ($x = 0, 0.33, 0.5, 0.67$ and 1)

S. Dimitrovska-Lazova^{1*}, D. Kovacheva², S. Aleksavska¹, M. Marinšek³, P. Tzvetkov²

¹ University “St. Cyril and Methodius”, Faculty of Natural Sciences and Mathematics,
Arhimedova 5, Skopje, R. Macedonia

² Institute of General and Inorganic Chemistry, Bulgarian Academy of Science,
“Acad. Georgi Bonchev” bl. 11, 1113 Sofia, Bulgaria

³ University of Ljubljana, Faculty of Chemistry and Chemical Technology,
Aškerčeva c. 5, 1000 Ljubljana, R. Slovenia

Received March 21, 2012; Revised May 2, 2012

Results on synthesis, structural investigations and the morphology of complex perovskites of general formula $\text{PrCo}_{1-x}\text{Cr}_x\text{O}_3$ (with $x = 0, 0.33, 0.5, 0.67$ and 1) are presented. The synthesis of the perovskites within this series was performed by solution combustion method using two different fuels: urea and glycine. The annealed samples were identified using X-ray powder diffraction. The purity of the compounds obtained using glycine as a fuel was better and for further investigations perovskites obtained with this fuel were used. The crystal structure was refined by the Rietveld method, and the morphology of the particles was investigated using SEM. All compounds within the series crystallize in $Pnma$ space group ($Z = 4$). The effect of the substitution of Co^{3+} ion with Cr^{3+} was investigated by analyzing different crystallochemical parameters (bond-lengths and tilt angles of the coordination octahedra, global instability index etc). A very interesting trend in changes of the structural distortion and global stability of the compounds in respect to x e.g. substitution of Co^{3+} with Cr^{3+} was found.

Key words: complex perovskites, XRD, SEM, crystallochemical calculations.

INTRODUCTION

Within the field of material science one of the most interesting groups of compounds belongs to perovskite structural type. Perovskite structure encompasses compounds with general formula ABX_3 , where A and B are cations and X is an anion. In the ideal perovskite structure the B-cation is coordinated by six anions in almost regular octahedron. The BX_6 octahedra are sharing same corners thus forming three-dimensional network of octahedral chains. The cavities formed by the octahedra are filled by A-cations which are cubooctahedrally coordinated by the anions. This kind of arrangement leads to cubic ($Pm3m$) structure [1, 2]. An important feature of perovskite structure is possible rotation (for small angle) of the BX_6 octahedra, while still retaining the chain-like connectivity. As a result, the symmetry of the structure is lowered to orthorhombic, monoclinic, hexagonal, etc. This structural flex-

ibility enables including almost all elements from the periodic table in the perovskite structure. So, there is great number of possible combinations of different cations in A and B positions, but also different anions in the X-position may be found, such as oxygen, halogen ions, cyanide group etc. Among these anions the most common are perovskites with oxide anion. Another important feature of the perovskite structure is the possibility for multiple substitutions in the positions of the cations, thus forming so-called complex perovskites. This possibility drastically enlarges the number of compounds with perovskite structure.

Depending on the nature of A and B cations and particular crystal structure, the physical and chemical properties of perovskites may vary in a wide range. Namely, in this group of compounds different physical and chemical properties emerge, namely: pyroelectricity, piezoelectricity, colossal magnetoresistance, catalytic activity, ferromagnetism, superconductivity etc. [1, 3]. From this point of view the perovskites containing cobalt ion in the B-position are intensively studied. Namely, cobalt-perovskites (RCoO_3) exhibit interesting properties

* To whom all correspondence should be sent:
E-mail: sandra@pmf.ukim.mk

such as high electronic conductivity [4], metal to insulator transition with increasing temperature [5], significant catalytic activity [3], specific magnetic properties [6–8], etc. Properties of cobaltates are tightly connected with some characteristics of cobalt ions such as the possibility to change the oxidation state (Co^{4+} , Co^{3+} , Co^{2+}) and also the possibility of altering the spin state of the Co^{3+} ion [7, 9, 10]. The change of the oxidation state of cobalt ion is usually triggered by substitutions in A or B positions (as in $\text{R}_{1-x}\text{Sr}_x\text{CoO}_3$) [11]. The spin state of the cobalt ion in compounds with rare earth metal in A-position has been a subject of investigation in a large number of studies [7, 9, 10, 12–16]. The spin state of Co^{3+} ion may change from low spin (LS) with t_{2g}^6 electron configuration, intermediate spin state (IS) with one electron in e_g -orbital ($t_{2g}^5e_g^1$) or high spin state (HS) with configuration $t_{2g}^4e_g^2$. It is expected that compounds with IS and HS state of the Co^{3+} ion to encounter Jahn-Teller distortion of the CoO_6 octahedra. At room temperature in most of the RCoO_3 perovskites (R is rare earth) Co^{3+} is in LS state. It is found that at room temperature the amount of IS Co^{3+} ions is the highest in LaCoO_3 , while it is smaller in PrCoO_3 [10]. Actually, with decreasing of the ionic radii of R^{3+} in the RCoO_3 series, the amount of the LS state of Co^{3+} ions is increasing [10, 16].

Continuing our investigation on different perovskites with cobalt ion [17, 18], in this work we present the synthesis of the perovskite series of general formula $\text{PrCo}_{1-x}\text{Cr}_x\text{O}_3$ (with $x = 0, 0.33, 0.5, 0.67$ and 1), the investigations of their crystal structure and some important crystallographic characteristics connected with the substitution of the cations in B position.

Although there is literature data [19–30] for the end members of the series (PrCoO_3 and PrCrO_3), any data about the solid solution between these two compounds have not been found yet. The literature data shows that PrCoO_3 and PrCrO_3 may be synthesized by different methods such as: solid state synthesis [7, 19, 20], decomposition of citrate precursor [21–24, 8, 11], synthesis based on complex precursors [25–29], self-propagating high temperature synthesis [30] and hydrothermal synthesis [30]. In this work the synthesis of Pr-perovskites by solution combustion method using two fuels – glycine and urea is presented.

It should be pointed out that the crystal structures of the end members of the series presented in this paper are already known. According to some literature data PrCoO_3 is cubic [19, 21, 24], but according to some others, it is orthorhombic [7, 8, 10, 11, 20, 22]. Some more detailed structural analysis of PrCoO_3 by XRD and neutron diffraction [11, 22] point out also that this compound crystallizes in the orthorhombic system (space group $Pnma$). The

crystal structure of PrCrO_3 was also reported [20, 26, 30, 31] as orthorhombic, space group $Pnma$. Taking these findings into consideration, it is expected that the new-synthesized complex perovskites of cobalt and chromium should crystallize in the orthorhombic system. Also, it is expected that the substitution of Co^{3+} ($r(\text{Co}^{3+}) = 0.545 \text{ \AA}$, LS) with chromium Cr^{3+} ion, which has slightly bigger ionic radii ($r(\text{Cr}^{3+}) = 0.615 \text{ \AA}$), would increase the lattice parameters and, consequently, the volume of the unit cell. In order to analyze the influence of substitution of Co^{3+} with Cr^{3+} on the crystal structure, the synthesized compounds were characterized by XRD and their crystal structure and several crystallographic parameters were calculated and compared. The morphology of the studied samples was also investigated by scanning electron microscopy (SEM).

EXPERIMENTAL

Synthesis

The synthesis of the $\text{PrCo}_{1-x}\text{Cr}_x\text{O}_3$ perovskites was performed by solution combustion method. For this purpose, nitrates of the constituting metals were used as starting materials. Calculated amounts of metal nitrates ($\text{Pr}(\text{NO}_3)_3 \cdot 6\text{H}_2\text{O}$, $\text{Co}(\text{NO}_3)_2 \cdot 6\text{H}_2\text{O}$ and $\text{Cr}(\text{NO}_3)_3 \cdot 9\text{H}_2\text{O}$) were dissolved in small amount of distilled water. The obtained solutions were thoroughly mixed on a stirrer. These solutions were used as starting mixtures in the combustion synthesis. The combustion syntheses were performed using two fuels: urea ($\text{CO}(\text{NH}_2)_2$) or glycine ($\text{NH}_2\text{CH}_2\text{COOH}$). The amounts of the fuels were calculated on the basis of propellant chemistry and were set to 1 [32]. The composition of the solutions varied according to the formula of the synthesized perovskite.

The synthesis of the perovskites using urea as a fuel was performed in the following manner: appropriate quantity of urea was dissolved in small amount of diluted nitric acid (1:1) and this solution was added to the particular mixture containing metal nitrates. After the homogenization of the solution it was transferred in muffle furnace. The mixture was slowly heated to temperature of $\sim 500 \text{ }^\circ\text{C}$. After the evaporation of water a vigorous combustion reaction started. In a very short time spongy powders were formed. Resulting materials were hand milled, transferred to ceramic dish and subjected to additional heating for 6 hours at $800 \text{ }^\circ\text{C}$.

The procedure using glycine as a fuel was just a little bit different. Glycine was dissolved in small amount of distilled water and this solution was added to pre-prepared mixture of metal nitrates solutions. The obtained mixture was heated at $80 \text{ }^\circ\text{C}$ under constant stirring. After the evaporation of

the water and gelatinization of the solution the vessel was transferred on a hot plate preheated above 300 °C. The gel boiled and after the evaporation of remaining water an initialization and combustion of the mixtures started. As a result, black (only in case of PrCrO₃ the product was green) spongy powders were formed. As-prepared samples were hand milled and calcined at 800 °C for 6 hours (2h and additional 4h).

XRD

The resulting powders were analyzed by X-ray diffraction. The XRD patterns were recorded on *Bruker D8 Advance* with Cu_{Kα} radiation and SolX detector within the range 10–120° 2θ at room temperature with step-scanning of 0.02°. The crystal structures were refined by the method of Rietveld using the Fullprof program [33].

SEM

The microstructure of the obtained compounds was investigated by SEM. Field-Emission FE-SEM Zeiss ULTRA PLUS microscope using accelerating voltage of 2kV was used. The samples were put onto graphite tape and were not gold sputtered prior to the microscopy. Images were taken using In-lens and/or standard Everhart-Thornley secondary electron (SE) detectors.

RESULTS AND DISCUSSION

As was mentioned in the experimental part, the solid solutions PrCo_{1-x}Cr_xO₃ ($x = 0, 0.33, 0.5, 0.67$)

and 1) were synthesized using both urea and glycine as a fuel. The recorded XRD patterns of the samples showed that in both cases perovskite compounds with same structure were obtained but the samples prepared using glycine as a fuel, were of better purity. This is illustrated by the XRD patterns (Fig. 1) for one of the members of the series (PrCo_{0.5}Cr_{0.5}O₃).

The XRD pattern on Figure 1a corresponds to PrCo_{0.5}Cr_{0.5}O₃ synthesized using urea and the others (Figs. 1b-d) using glycine as a fuel. Some impurities of Co₃O₄ could be detected in the compound obtained via urea (Fig. 1a), which are not present in the compound obtained at same temperature but via glycine (Fig. 1d). It should be mentioned that in the case of PrCo_{0.5}Cr_{0.5}O₃ the formation of the perovskite phase began right after the combustion of the initial mixture (as-synthesized sample, Fig. 1b) but by further heating on 800 °C a better crystallinity was obtained (Fig. 1b-d). Since the purity of the samples obtained using glycine was better than that using urea, the further investigations and discussion of the results were carried out on the samples synthesized by glycine.

The XRD patterns of the perovskite series PrCo_{1-x}Cr_xO₃ ($x = 0, 0.33, 0.5, 0.67$ and 1) obtained by the same synthetic route (heated 4 h on 800 °C) are presented on Figure 2.

As expected, the obtained compounds are isostructural and with perovskite structure. Namely, the obtained XRD patterns of the end members of the series, PrCoO₃ and PrCrO₃, are in accordance with the literature data [8, 22, 34]. Complex perovskites within the series show gradual shifting

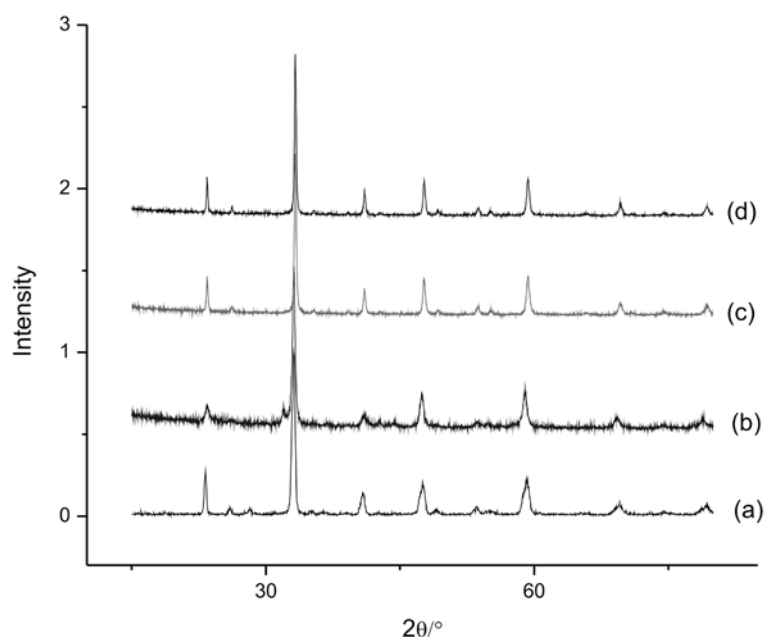


Fig. 1. XRD patterns of PrCo_{0.5}Cr_{0.5}O₃ obtained using (a) urea (heat treated for 6h at 800 °C), (b) glycine (as-synthesized) (c) glycine (after heat treatment for 2h at 800 °C), (d) glycine (after additional heat treatment for 4h at 800 °C)

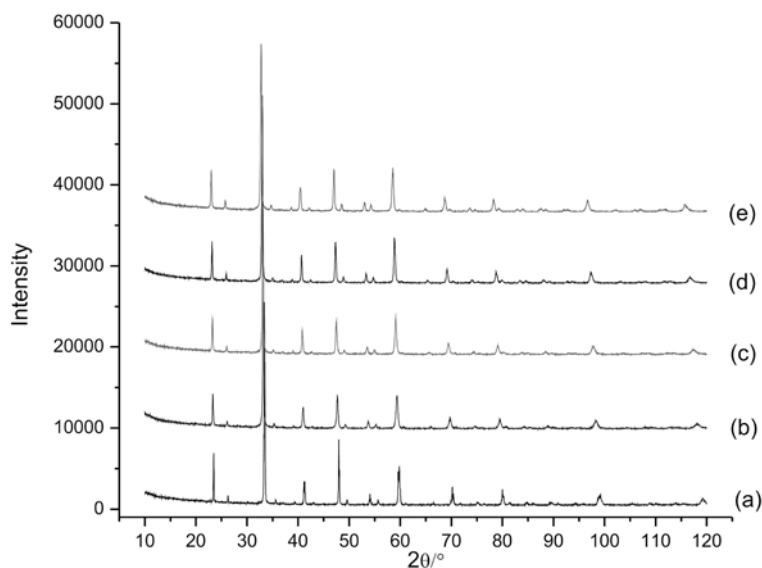


Fig. 2. XRD patterns of (a) PrCoO_3 , (b) $\text{PrCo}_{0.67}\text{Cr}_{0.33}\text{O}_3$, (c) $\text{PrCo}_{0.5}\text{Cr}_{0.5}\text{O}_3$, (d) $\text{PrCo}_{0.33}\text{Cr}_{0.67}\text{O}_3$, (e) PrCrO_3

Table 1. Unit cell parameters, $b/\sqrt{2}$, pseudo-cubic parameter a_p calculated using the equation $a_p = (V/Z)^{1/3}$ where Z is number of atoms in asymmetric unit and volume (V) of the unit cell

	$a/\text{Å}$	$b/\text{Å}$	$c/\text{Å}$	$(b/\sqrt{2})/\text{Å}$	$a_p/\text{Å}$	$V/\text{Å}^3$	ratio
PrCoO_3	5.34355(8)	7.57728(10)	5.37634(8)	5.3580	3.7896	217.6857	$c > b/\sqrt{2} > a$
$\text{PrCo}_{0.67}\text{Cr}_{0.33}\text{O}_3$	5.3834(3)	7.6139(4)	5.4027(4)	5.3838	3.8113	221.4495	$c > b/\sqrt{2} \approx a$
$\text{PrCo}_{0.5}\text{Cr}_{0.5}\text{O}_3$	5.4141(3)	7.6502(7)	5.4145(6)	5.4095	3.8274	224.2630	$a \approx c > b/\sqrt{2}$
$\text{PrCo}_{0.33}\text{Cr}_{0.67}\text{O}_3$	5.43702(20)	7.6750(3)	5.4292(2)	5.4270	3.8404	226.5558	$a > b/\sqrt{2} > c$
PrCrO_3	5.47897(10)	7.71528(16)	5.45127(11)	5.4555	3.8622	230.4349	$a > b/\sqrt{2} > c$

of the diffraction peaks towards smaller 2θ values with increasing of the value of x (Fig. 2), suggesting gradual increase of the substitution of cobalt ion. These results are in accordance with the expected changes in the XRD pattern in a case when smaller cation (Co^{3+}) is substituted with bigger one (Cr^{3+}).

As previously mentioned, the end members of the series, PrCoO_3 and PrCrO_3 , have GdFeO_3 -orthorhombic structure [8, 22, 34] and, accordingly, it was expected that all members of the series would be orthorhombic. The refinement of the crystal structures showed that all compounds crystallize in the orthorhombic space group $Pnma$, with four formula units per unit cell. The unit cell parameters, cell volumes, as well as, the pseudo-cubic parameter are presented in Table 1.

In aim to present the complete crystal structure of the newly synthesized members of the series, the Rietveld refinement approach was undertaken. The refinements were carried out using the structural model for PrCoO_3 as a starting model. For the intermediate structures it was assumed that the Co(III) and Cr(III) cations are randomly distributed in same crystallographic positions. The calculated and ob-

served patterns obtained by Rietveld refinement for one of the compounds ($\text{PrCo}_{0.5}\text{Cr}_{0.5}\text{O}_3$) is presented on Fig. 3 just as an example.

The fractional atomic coordinates and the discrepancy factors are presented in Table 2, and Table 3 presents selected distances and angles as well as the distortions of the coordination polyhedrons.

The values of the unit cell parameters of the end members of this series are in good agreement with the literature data [8, 22, 34]. Analyzing the changes of the unit cell parameters throughout the series and the relations between them, some interesting facts have arisen. Namely, as expected, the substitution of smaller Co^{3+} with slightly bigger Cr^{3+} increases the unit cell parameters, cell volumes, and the pseudo-cubic parameter a_p (Table 1). However, it is interesting to note the changes in the relationship between a and c parameters. As may be noticed from Figure 4, this relationship changes from $c > a$ (PrCoO_3 and $\text{PrCo}_{0.67}\text{Cr}_{0.33}\text{O}_3$) through $c \approx a$ ($\text{PrCo}_{0.5}\text{Cr}_{0.5}\text{O}_3$) to $c < a$ ($\text{PrCo}_{0.33}\text{Cr}_{0.67}\text{O}_3$ and PrCrO_3).

Obviously, in $\text{PrCo}_{1-x}\text{Cr}_x\text{O}_3$ series the decrease of the ionic radii of B-cation (from $r(\text{Cr}^{3+}) = 0.615 \text{ Å}$ to $r(\text{Co}^{3+}) = 0.545 \text{ Å}$) leads toward change in the

Fig. 3. Observed and calculated XRD patterns for $\text{PrCo}_{0.5}\text{Cr}_{0.5}\text{O}_3$ as well as their difference plot obtained by Rietveld refinement

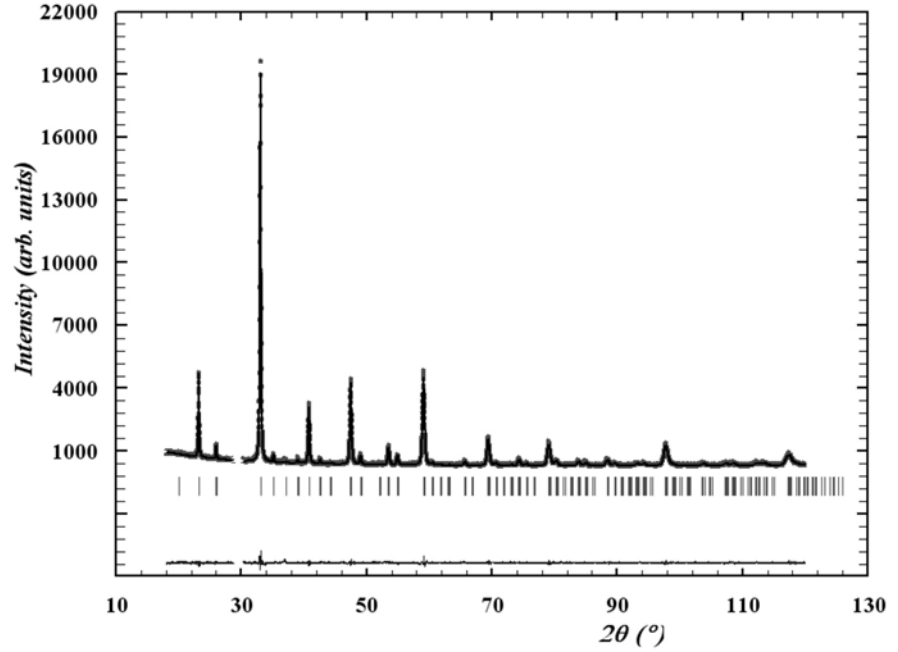


Table 2. Fractional atomic coordinates and discrepancy factors for $\text{PrCo}_{1-x}\text{Cr}_x\text{O}_3$ solid solution

Atoms	Param.	PrCoO_3	$\text{PrCo}_{0.67}\text{Cr}_{0.33}\text{O}_3$	$\text{PrCo}_{0.5}\text{Cr}_{0.5}\text{O}_3$	$\text{PrCo}_{0.33}\text{Cr}_{0.67}\text{O}_3$	PrCrO_3
Pr	x	0.02913(13)	0.02964(15)	0.03142(13)	0.03306(10)	0.03545(8)
	y	0.25	0.25	0.25	0.25	0.25
	z	0.9954(5)	0.9955(6)	0.9940(5)	0.9947(4)	0.9927(2)
	B	0.33(2)	0.29(3)	0.25(2)	0.292(19)	0.390(14)
Co/Cr	B	0.06(3)	0.18(4)	0.06(3)	0.12(3)	0.22(2)
O1	x	0.4947(15)	0.4893(16)	0.4864(15)	0.4897(14)	0.4869(10)
	y	0.25	0.25	0.25	0.25	0.25
	z	0.060(2)	0.054(3)	0.060(3)	0.072(4)	0.0643(18)
	B	1.9(4)	0.2(6)	0.6(7)	0.9(6)	0.9(3)
O2	x	0.274(2)	0.282(3)	0.288(3)	0.294(2)	0.2905(13)
	y	0.0388(14)	0.0420(17)	0.0353(16)	0.0364(14)	0.0428(10)
	z	0.7138(19)	0.700(3)	0.701(3)	0.7086(19)	0.7101(13)
	B	0.9(3)	1.8(3)	0.9(3)	0.9(3)	1.04(16)
R	$R_p/\%$	14.6	13.8	11.3	10.3	7.74
	$R_{wp}/\%$	10.7	11.9	10.4	9.86	8.66
	$R_{exp}/\%$	9.45	9.50	8.98	8.50	7.72
	χ^2	1.28	1.56	1.34	1.35	1.26
	$R_B/\%$	3.09	2.33	1.88	2.14	1.68

relationship of the unit cell parameters from $a < c$ to $c > a$. This a/c relationship points out to the reasons for distortion of perovskite structure. Namely, it is known that the transition from cubic to orthorhombic structure ($Pnma$) due to the tilting of the octahedra leads to unit cell with $c < a$. The inverse relationship, $a < c$ is characteristic for perovskites in which additional distortion of the BO_6 octahedrons appears [10]. In this series, the additional distortion appears in cases when the content of Co^{3+} prevails

that of Cr^{3+} , such as in $\text{PrCo}_{0.67}\text{Cr}_{0.33}\text{O}_3$. This additional octahedral distortion may also be noticed from the comparison of a , $b\sqrt{2}$ and c (Table 1). It is interesting to point out that only in PrCrO_3 and $\text{PrCo}_{0.33}\text{Cr}_{0.67}\text{O}_3$ the relation between these parameters is $a > b\sqrt{2} > c$ as in the O-type perovskites. In this type of perovskites the octahedral tilting is primarily the only distortional mechanism and the lattice distortion is small. In $\text{PrCo}_{0.5}\text{Cr}_{0.5}\text{O}_3$ a and c parameters are almost identical, $a \approx c > b/\sqrt{2}$ and this perovskite

Table 3. Values of Pr-O and B-O distances, average $\langle\text{Pr-O}\rangle$ distances in twelve coordinated praseodymium and average distance in BO_6 octahedra, Δ_{12} , Δ_{10} and Δ_6 , B-O1-B and B-O2-B angles

	PrCoO_3	$\text{PrCo}_{0.67}\text{Cr}_{0.33}\text{O}_3$	$\text{PrCo}_{0.5}\text{Cr}_{0.5}\text{O}_3$	$\text{PrCo}_{0.33}\text{Cr}_{0.67}\text{O}_3$	PrCrO_3
Pr-O1	2.877(8)	2.926(9)	2.972(8)	2.984(8)	3.031(6)
	2.512(8)	2.495(9)	2.489(8)	2.518(8)	2.504(6)
	2.992(11)	2.977(16)	3.010(16)	3.09(2)	3.048(10)
	2.397(11)	2.444(16)	2.427(16)	2.36(2)	2.430(10)
Pr-O2 x 2	2.562(11)	2.627(15)	2.673(15)	2.667(11)	2.623(7)
	2.384(11)	2.324(15)	2.356(14)	2.365(11)	2.362(7)
	3.140(11)	3.235(15)	3.238(15)	3.254(11)	3.304(7)
	2.697(11)	2.682(14)	2.641(14)	2.658(11)	2.723(8)
$\langle\text{Pr-O}\rangle_{12}$	2.6953	2.7148	2.7262	2.7367	2.7531
Δ_{12}	9.9624	12.429	12.39	13.46	14.06
Δ_{10}	5.7991	6.5998	6.917	8.18	7.885
B-O1 x 1	1.9218(18)	1.927(2)	1.941(3)	1.959(4)	1.9617(18)
B-O2 x2	1.885(11)	1.891(16)	1.921(16)	1.979(11)	1.988(7)
	1.978(10)	2.026(16)	2.003(16)	1.958(11)	1.981(7)
$\langle\text{B-O}\rangle$	1.9283	1.948	1.955	1.9653	1.9769
Δ_6	0.3933	0.8586	0.3189	0.0242	0.0316
B-O1-B	160.6	162.24	160.24	156.74	158.98
B-O2-B	157.8	153.6	154.7	154.7	153.6

is orthorhombic with pseudo-tetragonal unit cell. In the last two members (PrCoO_3 and $\text{PrCo}_{0.67}\text{Cr}_{0.33}\text{O}_3$) the ratio between the unit cell parameters changes to $c > b/\sqrt{2} > a$, which also highlights some additional distortion of the octahedra. It is interesting to compare these results with structural changes in RCoO_3 (R = lanthanide) series [7, 22], where the change in the mutual relationship between a and c parameters (from $a > c$ to $c > a$) is driven by the increasing of the ionic radii of A-cation. This change ends with change in symmetry from orthorhombic to rhombohedral (at LaCoO_3).

Taking into consideration these changes in the unit cell parameters relationship due to the $\text{Co}^{3+}/\text{Cr}^{3+}$ sub-

stitution an additional crystallochemical calculations were done. Also, it seemed interesting to examine the possibility of changes in morphology and dimensions of the crystals obtained by $\text{Co}^{3+}/\text{Cr}^{3+}$ substitution in the perovskite structure.

The distortion of the octahedra may be parameterized by the bond-length distortion of the octahedra, Δ_6 , calculated using the equation: $\Delta = \Sigma[(r_i - r)/r]/n \cdot 10^3$ (Table 3). As was pointed out previously, the calculated Δ_6 values for PrCoO_3 and $\text{PrCo}_{0.67}\text{Cr}_{0.33}\text{O}_3$ are higher and are emphasizing an increased distortion of the octahedra. The maximal Δ_6 is found in $\text{PrCo}_{0.67}\text{Cr}_{0.33}\text{O}_3$ and throughout the complex perovskites in the series,

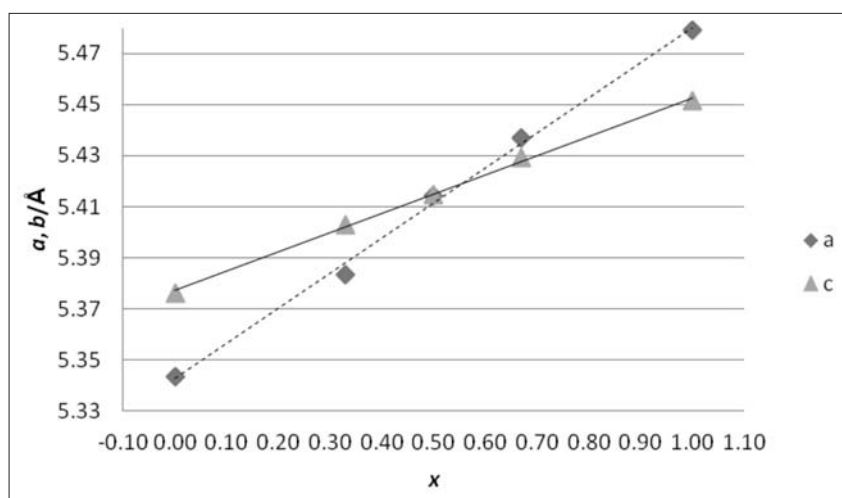


Fig. 4. The change of the relation between the unit cell parameters a and c in $\text{PrCo}_{1-x}\text{Cr}_x\text{O}_3$ with increasing of x ($x = 0, 0.33, 0.5, 0.67$ and 1)

the Δ_6 is decreasing. Analyzing the values of the particular B-O distances, two facts may be noticed. Firstly, the distances between the B cation and the O1 anions are increasing from PrCoO_3 to PrCrO_3 . This trend is the same for B-O2 distances, although not so regular. More careful examination of the values of these distances shows that at the beginning of the series the first from the two B-O2 distances is longer, while at the end of the series (at PrCrO_3) the second one is shorter than the first one. Bearing in mind that the B-O2 distances are along a and c axes the interchange of these distances is in accordance with the change of the a/c relationship.

Contrary to the direction of the changes in bond-length distortion of the BO_6 polyhedra, the distortion of the coordination polyhedra of the A cation is increasing with increasing of the amount of chromium ion e.g. with increasing of x (Table 3). The average $\langle\text{Pr-O}\rangle_{12}$ distances for twelve coordinated Pr are increasing from 2.6953 Å in PrCoO_3 to 2.7531 Å at PrCrO_3 . This change influences the coordination around Pr-cation. Namely, starting from $\text{PrCo}_{0.67}\text{Cr}_{0.33}\text{O}_3$ two of the Pr-O2 distances are too long to be encountered as a part of the coordination of Pr^{3+} , and probably the coordination number of praseodymium changes to 10. This change in the coordination of praseodymium is expressed in high values of the distortion parameters Δ_{12} . More precisely, these values are significantly higher than the values for Δ_{10} in all compounds except in PrCoO_3 , suggesting change in coordination sphere from 12 to 10.

The deviation from the ideal cubic perovskite structure may be also described by the observed so called tolerance factor, t_0 [35]. This factor represents the ratio between the average $\langle\text{Pr-O}\rangle_{12}$ and $\langle\text{B-O}\rangle_6$ distances and is calculated by the equation: $t_0 = \langle\text{Pr-O}\rangle_{12}/\sqrt{2} \langle\text{B-O}\rangle_6$. The observed tolerance factor is related with the degree of the octahedral tilting. The values close or equal to 1 corresponds to the structures without tilting of the octahedra [36]. In order to check the trend of changes of the observed

tolerance factors in relation with tilting within this perovskite series, the tilt angles θ , φ and Φ were calculated (Table 4).

These tilt angles represents the rotation of the octahedra around $[110]_p$, $[001]_p$ and $[111]_p$ pseudo-cubic axes and are calculated using the fractional atomic coordinates [2]. It may be noticed that in the structure of PrCoO_3 the value of t_0 (calculated assuming coordination number 12 for A cation, $t_{o(12)}$, and 10 $t_{o(10)}$) is closer to 1 and this compound has the smallest tilt angles. The values of t_0 are increasing throughout the series, with increasing of x , and also the tilting of the octahedra is more pronounced (θ , φ and Φ , Table 4). These results are also in accordance with the values of the tilt angles calculated on the bases of the experimental B-O1-B and B-O2-B angles, using the formula $\varphi^* = (180 - \langle\text{B-O1,2-B}\rangle)/2$, where $\langle\text{B-O1,2-B}\rangle$ is the average value of B-O1,2-B angles (Table 4). Obviously, in complex perovskites, the tilt angles of the octahedra are increasing with increasing of x , e.g. of the substitution of Co^{3+} with Cr^{3+} . These values suggest that the overlap of the oxygen orbitals with the orbitals of the B cation is smaller. Namely, as this angle deviates more from 180° smaller orbital overlap is achieved [11].

In order to evaluate the overall distortion of the perovskite structure in the series, additional distortion parameters were also calculated: orthorhombic distortion, spontaneous strain (s), d-cell distortion (Table 4). These parameters are calculated using the unit cell parameters and they pointed out to the change in the type of the distortion. It may be concluded that these values are diminishing from PrCoO_3 to $\text{PrCo}_{0.5}\text{Cr}_{0.5}\text{O}_3$, (the smallest value) and then they start rising again.

According to the previous discussion it may be concluded that there are two types of distortions in the structures of the members of this perovskite series. In PrCoO_3 and $\text{PrCo}_{0.67}\text{Cr}_{0.33}\text{O}_3$, in which the content of Co^{3+} prevails the content of Cr^{3+} , the octahedra are more distorted in respect to the bond

Table 4. Change of values of several crystallographic parameters throughout the series. Calculated parameters are: orthorhombic distortion [35], spontaneous strain (s) [2], d-cell distortion [7], Global Instability index (GII) [2], observed tolerance factors $t_{o(12)}$ and $t_{o(10)}$ [2], tilt angles calculated using fractional atomic coordinates [2] and tilt angle obtained from B-O1,2-B angles

	Orthorhombic distortion	Spontaneous strain (s)	d-cell distortion	GII	$t_{o(12)}$	$t_{o(10)}$	Tilt angles			
							θ	φ	Φ	φ^*
PrCoO_3	0.0171	-0.0061	0.0626	0.2112	0.9884	0.9558	9.700	7.012	11.950	10.4
$\text{PrCo}_{0.67}\text{Cr}_{0.33}\text{O}_3$	0.0112	-0.0036	0.0279	0.2225	0.9855	0.9477	8.879	9.538	13.004	11.04
$\text{PrCo}_{0.5}\text{Cr}_{0.5}\text{O}_3$	0.0072	$-7.4 \cdot 10^{-5}$	0.0018	0.1967	0.9860	0.9490	9.880	9.948	13.985	11.265
$\text{PrCo}_{0.33}\text{Cr}_{0.67}\text{O}_3$	0.0963	0.0014	0.0062	0.1812	0.9846	0.9474	11.630	9.697	15.099	12.14
PrCrO_3	0.2341	0.0051	0.0497	0.0762	0.9847	0.9453	10.509	9.136	13.891	11.855

lengths. This leads to bigger instability and stress in the structure, which are expressed in the high values of GII (global instability index, Table 4). These high values (> 0.2 valence units) of GII, point out to big strain in these structures. This type of distortion may be connected with possible existence of Co^{3+} ion in intermediate spin (IS) state. Namely, the IS would increase the deformation of the octahedra as a result of appearance of Jahn-Teller distortion.

In $\text{PrCo}_{0.33}\text{Cr}_{0.57}\text{O}_3$ and PrCrO_3 , in which the content of Cr^{3+} prevails the content of Co^{3+} the distortion is mainly due to the rotation of the octahedra, while the bond-lengths distortion of the octahedra is significantly smaller. The most stable structure is that of $\text{PrCo}_{0.5}\text{Cr}_{0.5}\text{O}_3$. It seems that the effects of the

bond-lengths distortion and tilting of the octahedral act in opposite directions in this perovskite series, leading to stabilization of the structure.

In aim to check the influence of these structural changes due to partial substitution of the cations in B-position, on their morphology, SEM images of the perovskites of this series were recorded. Figure 5 shows the SEM micrographs of $\text{PrCo}_{1-x}\text{Cr}_x\text{O}_3$ powders obtained by heat treatment at 800°C for 4 hours.

The images show single perovskite phases with appropriate nanosize crystallinity. The porous structure implies the outflow of gases produced by decomposition of nitrates and combustion of glycine. As can be seen, the morphology of the compounds within the series is very similar.

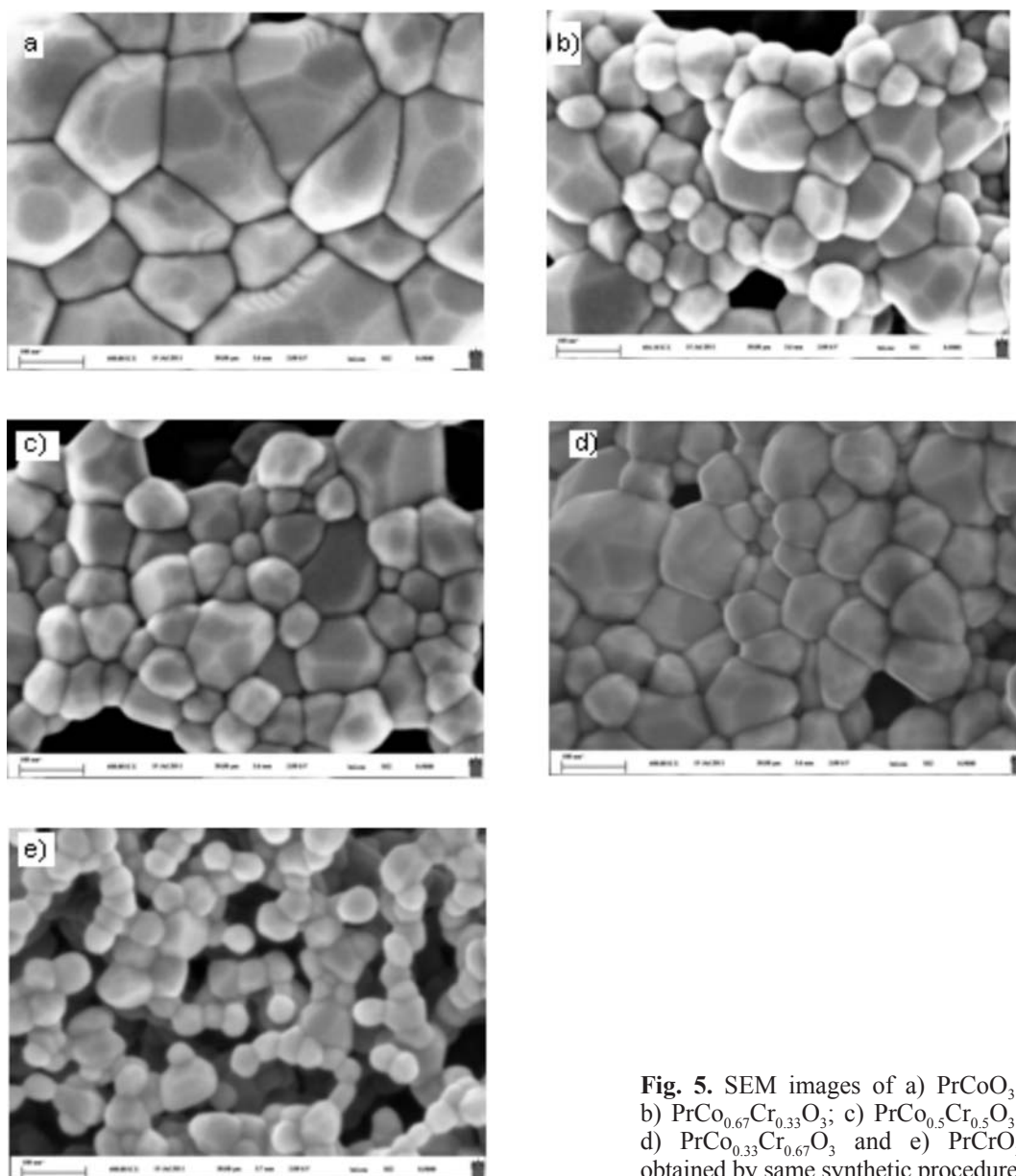


Fig. 5. SEM images of a) PrCoO_3 ; b) $\text{PrCo}_{0.67}\text{Cr}_{0.33}\text{O}_3$; c) $\text{PrCo}_{0.5}\text{Cr}_{0.5}\text{O}_3$; d) $\text{PrCo}_{0.33}\text{Cr}_{0.67}\text{O}_3$ and e) PrCrO_3 obtained by same synthetic procedure

CONCLUSION

The perovskites within the series $\text{PrCo}_{1-x}\text{Cr}_x\text{O}_3$ were obtained by solution combustion method using urea or glycine as a fuel. The purity of the samples obtained using glycine was better than that using urea, so the further investigations were carried out on the samples synthesized by glycine. The Rietveld refinement of the crystal structures showed that all compounds within this series crystallize in the orthorhombic space group *Pnma* with four formula units per unit cell.

In aim to study the influence of $\text{Co}^{3+}/\text{Cr}^{3+}$ substitution on the perovskite structure, several crystallochemical parameters were calculated. The detailed analysis of structural changes due to substitution of Co^{3+} with Cr^{3+} revealed some interesting features. Thus, it was concluded that in perovskites where the content of Co^{3+} prevails that of Cr^{3+} (PrCoO_3 and $\text{PrCo}_{0.67}\text{Cr}_{0.33}\text{O}_3$), except the distortion due to octahedral tilting the octahedral distortion in respect to the bond lengths is also significant. This leads to bigger instability and stress in the structure, which are expressed in the high values of GII. In $\text{PrCo}_{0.33}\text{Cr}_{0.57}\text{O}_3$ and PrCrO_3 , in which the content of Cr^{3+} prevails the content of Co^{3+} the distortion is mainly due to the octahedral tilting. The most stable structure is that of $\text{PrCo}_{0.5}\text{Cr}_{0.5}\text{O}_3$.

Acknowledgement: The authors thank the National Science Fund of Bulgaria and the Ministry of Education and Science of Republic of Macedonia for the financial support under contract DNTS/Macedonia 01/7/08.12.2011.

REFERENCES

1. F. S. Galasso, Perovskites and High Tc Superconductors, Gordon and Breach Science Publishers, 1990.
2. R. H. Mitchell, Perovskites: Modern and Ancient, Almaz press – Thunder Bay, 2002.
3. M. A. Peña, J. L. G. Fierro, *Chem. Rev.*, **101**, 1981 (2001).
4. T. Ishihara (Ed), Perovskite Oxide for Solid Oxide Fuel Cells (Fuel Cells and Hydrogen Energy), Springer, Dordrecht, 2009.
5. S. Yamaguchi, Y. Okimoto, Y. Tokura, *Phys. Rev. B*, **54**, R11022 (1996).
6. A. Fondado, J. Mira, J. Rivas, C. Rey, M. P. Breijo, and M. A. Señaris-Rodríguez, *J. App. Phys.*, **87**(9), 5612 (2000).
7. K. Knížek, Z. Jirák, J. Hejtmánek, M. Veverka, M. Maryško, G. Maris, T. T. M. Palstra, *Eur. Phys. J. B*, **47**, 213 (2005).
8. H. W. Brinks, H. Fjellvåg, A. Kjekshus, B. C. Hauback, *J. Solid State Chem.*, **147**, 464 (1999).
9. J.-Q. Yan, J.-S. Zhou, J. B. Goodenough, *Phys. Rev. B*, **69**, 134409 (2004).
10. J.-S. Zhou, J.-Q. Yan, J. B. Goodenough, *Phys. Rev. B*, **71**, 220103R (2005).
11. G.Ch. Kostoglouidis, N. Vasilakos, Ch. Ftikos, *Solid State Ionics*, **106**, 207 (1998).
12. A. P. Sazonov, I. O. Troyanchuk, V. V. Sikolenko, *Crystallogr. Rep.*, **51**, 11 (2006).
13. T. Fujita, T. Miyashita, Y. Yasui, Y. Kobayashi, M. Sato, E. Nishibori, M. Sakata, Y. Shimojo, N. Igawa, Y. Ishii, K. Kakurai, T. Adachi, Y. Ohishi, M. Takata *J. Phys. Soc. Jpn.*, **73**, 1987 (2004).
14. X. G. Luo, X. Li, G. Y. Wang, G. Wu, X. H. Chen, *J. Solid State Chem.*, **179**, 2175 (2006).
15. R. Caciuffo, D. Rinaldi, and G. Barucca, J. Mira, J. Rivas, M. A. Señaris-Rodríguez, P. G. Radaelli, D. Fiorani, J. B. Goodenough, *Phys. Rev. B*, **59**, 1068 (1999).
16. G. Thornton, F. C. Morrison, S. Partington, B. C. Tofield, D. E. Williams, *J. Phys. C: Solid State Phys.*, **21**, 2871 (1988).
17. S. Dimitrovska-Lazova, D. Kovacheva, S. Aleksovska, V. Mirceski, *Proceedings of 45th Meeting of Serbian Chemical Society*, Novi Sad, 2007.
18. S. Dimitrovska-Lazova, V. Mirceski, D. Kovacheva, S. Aleksovska, *J. Solid State Electrochemistry*, **16**, 219 (2012).
19. V. V. Kharton, E. N. Naumovich, A. A. Vechev, A. V. Nikolaev, *J. Solid State Chem.*, **120**, 128 (1995).
20. S. Pal, S. H'ebert, C. Yaicle, C. Martin, A. Maignan, *Eur. Phys. J. B*, **53**, 5 (2006).
21. J. L. G. Fierro, M. A. Pena, L. Gonzalez Tejuca, *J. Mater. Sci.*, **23**, 1018 (1988).
22. J. A. Alonso, M. J. Martínez-Lope, C. de la Calle, V. Pomjakushin, *J. Mater. Chem.*, **16**, 1555 (2006).
23. J.-W. Moon, Y. Masuda, W.-S. Seo, K. Koumoto, *Mater. Sci. Eng.*, **B85**, 70 (2001).
24. Y. Ren, B. Li, J. Wang, X. Xu, *J. Solid State Chem.*, **177**, 3977 (2004).
25. P. S. Devi, M. S. Rao, *J. Therm. Anal.*, **48**, 909 (1997).
26. P. S. Devi, *J. Mater. Chem.*, **3**, 373 (1993).
27. P. A. Brayshaw, A. K. Hall, W. T. A. Harrison, J. M. Harrowfield, D. Pearce, T. M. Shand, B. W. Skelton, C. R. Whitaker, A. H. White, *Eur. J. Inorg. Chem.*, 1127 (2005).
28. Y. Sadaoka, E. Traversa, M. Sakamoto, *J. Mater. Chem.*, **6**, 1355 (1996).
29. Y. Seto, K. Umamoto, T. Aarii, Y. Masuda, *J. Therm. Anal. Calorim.*, **76**, 165 (2004).
30. M. V. Kuznetsov, Ivan P. Parkin, *Polyhedron*, **17**, 4443 (1998).
31. K. Sardar, M. R. Lees, R. J. Kashtiban, J. Sloan, R. I. Walton, *Chem. Mater.*, **23**, 48 (2011).
32. M. M. A. Sekar, K. C. Patil, *J. Mater. Chem.*, **2**, 739 (1992).
33. J. Rodriguez-Carvajal, *Physica B*, **192**, 55 (1993).
34. S. Geller, *Acta Crystallogr.*, **10**, 243 (1957).
35. G. Huo, D. Song, Q. Yang, F. Dong, *Ceram. Int.*, **34**, 497 (2008).
36. Sasaki, C. T. Prewitt, J. D. Bass, W. A. Schulze, *Acta Crystallogr.*, **C43**, 1668 (1987).
37. C. L. Bull, P. F. McMillan, *J. Solid State Chem.*, **177**, 2323 (2004).

СИНТЕЗ И СТРУКТУРНИ ДЕТАЙЛИ НА ПЕРОВСКИТИ ОТ СЕРИЯТА
PrCo_{1-x}Cr_xO₃ (x = 0, 0.33, 0.5, 0.67 и 1)

С. Димитровска-Лазова^{1*}, Д. Ковачева², С. Алексовска¹,
М. Маринчек³, П. Цветков²

¹ Университет „Св. Кирил и Методиј“, Факултет по Естествени науки и Математика,
Архимедова 2, Скопје, Македонија

² Институт по опща и неорганична химия, Българска академия на науките,
„Акад. Г. Бончев“ бл.11, София, България

³ Университет на Люблиана, Факултет по химия и химични технологии,
Aškerčeva c. 5, 1000 Люблиана, Словения

Постъпила на 21 март, 2012 г.; приета на 2 май, 2012 г.

(Резюме)

Представен е синтез, структурно изследване и морфология на комплексни перовскити с обща формула PrCo_{1-x}Cr_xO₃ (with x = 0, 0.33, 0.5, 0.67 и 1). Получените перовскити са синтезирани по метода на комбустия през разтвор с използване на два вида гориво: урея и глицин. Накалените образци са идентифицирани с прахова рентгенова дифракция. Получените съединения с глицин като гориво са с по-голяма чистота и за изследване бяха използвани образци синтезирани с това гориво. Кристалната структура беше уточнена по метода на Ритвелд, а морфологията на частиците характеризирани със SEM. Всички съединения от серията кристализират в пространствена група *Pnma* (Z = 4). Ефекта от заместване на Co³⁺ с Cr³⁺ е изследван с анализ на различни кристалохимични параметри (дължина на връзки и ъгли на накланяне на координационните октаедри, глобален индекс на нестабилност и др.). беше установена интересна промяна в дисторзията на структурата и глобалният индекс на стабилност в зависимост от степента на заместване на Co³⁺ с Cr³⁺.